New Airfoil Design Concept

Preston A. Henne* and Robert D. Gregg III†
Douglas Aircraft Company, McDonnell Douglas Corporation, Long Beach, California 90846

This article summarizes the development of a new airfoil design concept. The new concept is based on utilizing unconventional geometry characteristics near the airfoil trailing edge. These characteristics include a finite trailing-edge thickness, strongly divergent trailing-edge upper and lower surfaces, and high surface curvature on the lower surface at or near the lower surface trailing edge. The article includes the original development of the new concept, computational analyses of airfoils and a wing utilizing the concept, airfoil validation wind-tunnel test results of several configurations, and wing validation wind-tunnel test results for a complete wing design. In addition to validating the concept, the airfoil and wing testing provided additional detailed data to better understand the aerodynamic advantage of such an unconventional trailing-edge configuration. It is demonstrated that the concept represents an advancement in airfoil technology beyond that achieved with the supercritical airfoil. This concept provides the aerodynamicist an additional degree of design freedom and flexibility previously unrecognized.

Introduction

THE aerodynamic design of airfoil sections continues today as an elegant yet practical engineering design problem. Elegant in that the solution of any airfoil design problem, however complex the problem, is nothing more than a two-dimensional closed contour. Practical in that many, if not most, problems in aerodynamics involve the generation of lift, drag, and moment by airfoil sections.

The airfoil design problem has received much attention in experimental, theoretical, and computational studies. Numerous volumes and documents have been compiled to summarize such studies. Reference 1 stands as a classic example of such documentation and provides an excellent summary of early airfoil research efforts. Early theoretical studies of airfoil design led to the decomposition of airfoil geometric characteristics into thickness, camber, and angle of attack, as shown in Fig. 1. Much of the early design studies dealt with the proper combination thickness shapes and camber shapes necessary to achieve some aerodynamic design goal. It is interesting to point out that few studies were focused on details associated with the airfoil trailing edge. Trailing-edge effects normally were of concern only when mechanical variations for high-lift systems or control systems were introduced.[1,2]

Traditionally, airfoil closure has been accomplished by using trailing-edge included angles, typically in the 5–15 deg range, in conjunction with essentially zero trailing-edge thickness. Early trailing-edge design principles were that the trailing edge must be sharp, to avoid drag penalties, and the trailing-edge included angle, as defined by ϵ in Fig. 1, must be positive, to allow for practical manufacture. These principles caused most early airfoil trailing-edge geometries to be wedge shaped.

More recently, work by Whitcomb[3] and others to develop the supercritical airfoil has shown the possibility of using a thin trailing-edge geometry with near-parallel trailing-edge surfaces to produce a superior transonic airfoil section. The thin trailing-edge and high aft-camber geometry provides for significant aft lift-loading on the supercritical airfoil, as indicated in Fig. 2. The aft loading represents a large increment in lift and contributes a major part of the transonic performance improvement associated with the supercritical airfoil.

Early analysis and critique of the supercritical airfoil revealed several adverse characteristics. First, the thin aft section introduced concern about structural penalties of the thin highly loaded trailing-edge configuration. Subsequent research, summarized in Ref. 4, provides a conclusion that a small amount of trailing-edge thickness or bluntness can be incorporated with little or no drag penalty. Such a trailing-edge thickness, less than 1% chord, is small but nevertheless alleviates concern for practical manufacturability. Applications of the supercritical airfoil have generally made use of this trailing-edge bluntness approach to achieve essentially parallel upper and lower surfaces in a practical design. Second, adverse viscous boundary-layer effects have been found to be more significant for highly aft-loaded airfoils.[5] A significant amount of the aft camber is effectively lost due to boundary-layer decambering near the upper surface trailing edge and in the lower surface concave region. As a result of these adverse characteristics, the full theoretical benefit of the supercritical airfoil is not obtained in practice.

Fundamental airfoil research efforts have identified a third type of trailing edge that provides superior aerodynamic performance compared to the previous types of closures. This new trailing-edge concept utilizes three fundamental characteristics. First, a finite trailing-edge thickness is required. Second, strongly divergent trailing-edge upper and lower surfaces are introduced. Third, the surface curvature on the lower surface increases rapidly as the trailing edge is approached. The combination of these three characteristics produces an unconventional airfoil trailing edge, as shown in Fig. 3. This type of airfoil is referred to as a divergent trailing edge (DTE) airfoil (United States Patent No. 4,858,852).

Origin of the Concept

The origin of this new concept in airfoil design is attributed to a two-part design study using computational aerodynamics in 1981. The first part of the 1981 study involved an analysis of the blunt trailing-edge effects reported in Ref. 4. The transonic airfoil analysis method of Bauer, Garabedian, and Korn, referred to as *Pgm H*,[6] was used to calculate the aerodynamic characteristics of the airfoil sections reported in Ref. 4. The *Pgm H* method utilizes an integral boundary-layer solution in conjunction with the profile drag formula of Squire and Young to evaluate viscous drag characteristics. This combination is quite reasonable for the drag created by airfoil

Received May 25, 1989; presented as Paper 89-2201 at the AIAA 7th Applied Aerodynamics Conference, Seattle, WA, July 31–Aug. 2, 1989; revision received June 28, 1990; accepted for publication June 29, 1990.

*Principal Staff Engineer, Senior, Aerodynamics and Acoustics Subdivision; currently Deputy General Manager, MD-90/MD-80 Product Definition. Associate Fellow AIAA.

†Section Manager, Aerodynamic Design, Aerodynamics and Acoustics Subdivision. Member AIAA.

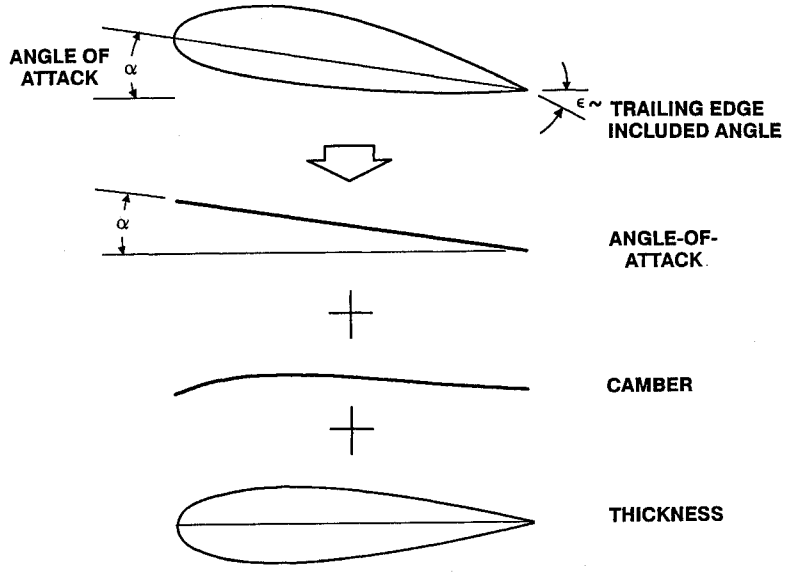

Fig. 1 Classical airfoil decomposition into angle of attack, camber, and thickness.

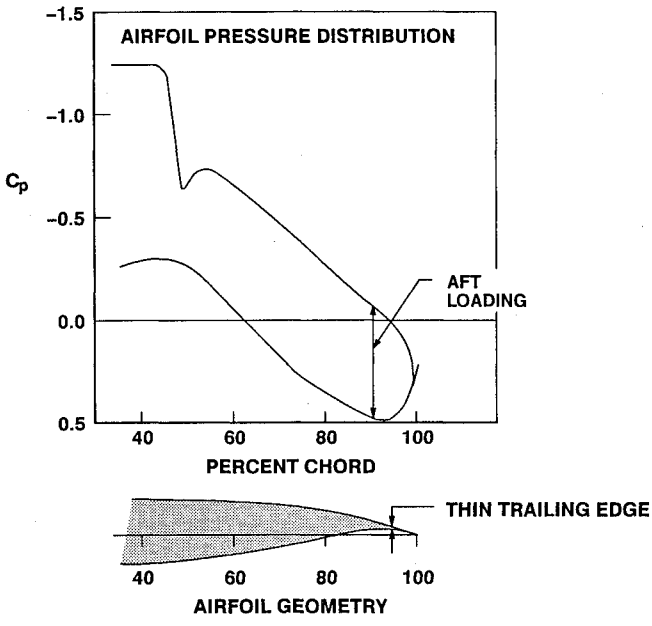

Fig. 2 Supercritical airfoil aft loading and trailing-edge geometry.

upper and lower surfaces. However, a major shortcoming of the original *Pgm H* was the inability of the numerical scheme to evaluate base drag. In order to address the base drag characteristics, a semiempirical base drag formula was developed. The formula for incremental base drag coefficient is

$$C_{d_{\text{base}}} = -C_{p_{\text{base}}} \frac{q_{te}}{q_o} \frac{\Delta Z_{te}}{C} \tag{1}$$

where $C_{p_{\text{base}}}$ is the base pressure coefficient, referenced to local potential flow conditions at the trailing edge; q_{te}/q_o is the local to freestream dynamic pressure ratio; and $\Delta Z_{te}/C$ is the nondimensional trailing-edge thickness parameter. The key to this formula is determining the base pressure coefficient. The correlations of Nash[7] are used for this purpose. The interesting facet of this approach is that, for trailing-edge thickness values less than about 4%, the Nash data indicate a linear variation of base pressure coefficient with trailing-edge thickness. This linearity substituted into Eq. (1) results in

$$C_{d_{\text{base}}} \sim \left(\frac{\Delta Z_{te}}{C}\right)^2 \tag{2}$$

The quadratic variation of the base drag increment with trailing-edge thickness, as indicated by Eq. (2), leads to the expec-

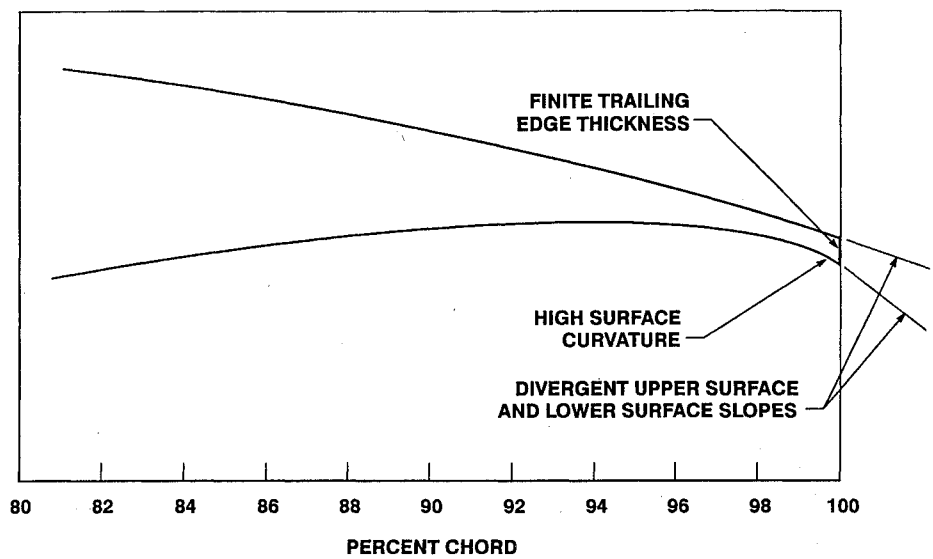

Fig. 3 Divergent trailing-edge airfoil geometry.

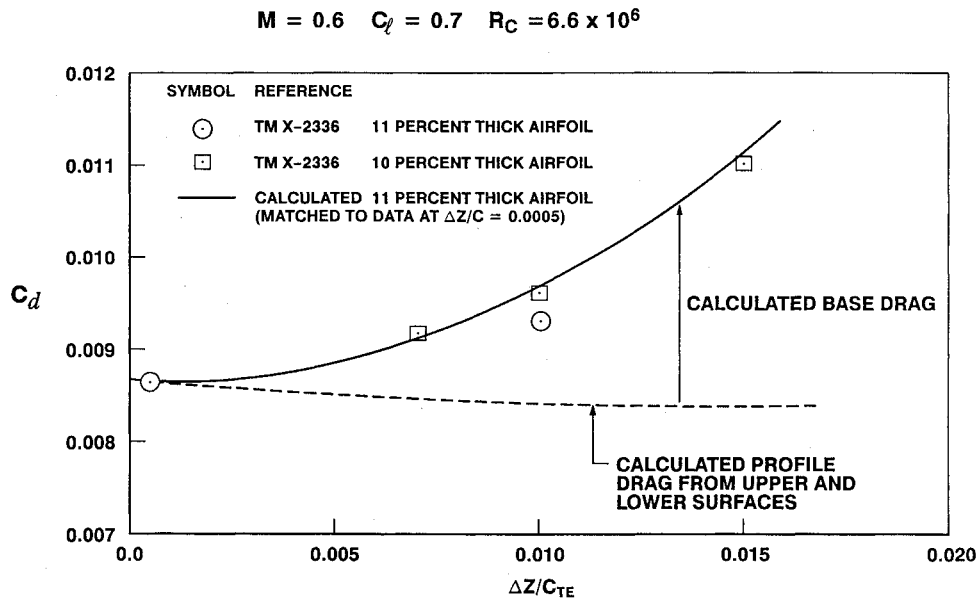

Fig. 4 Comparison of calculated and measured section drag variation with trailing-edge thickness.

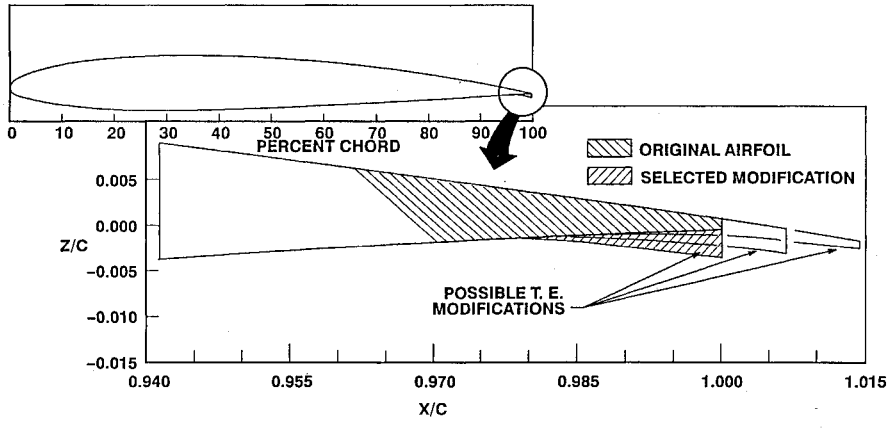

Fig. 5 Possible trailing-edge modifications for DSMA 661 1981 study case.

tation that the base drag penalty for small trailing-edge thicknesses might indeed be negligible.

This formula, when combined with *Pgm H* calculations, provided the drag comparison shown in Fig. 4. In this figure, the measured drag variation with trailing-edge thickness[4] is compared to the calculated variation. The calculated drag has been shifted lower by several counts to match the data point for the thinnest trailing edge. The dashed line indicates the basic profile drag variation stemming from the Squire and Young calculation. It reveals an interesting but modest reduction in drag with increasing trailing-edge thickness. This effect is related to an increase in local velocites near the trailing edge as a result of the additional local thickness. The quadratic base drag increment added to this basic level is also shown. The calculated variation in drag with trailing-edge thickness matches the measured results remarkably well for drag data. The comparison indicates that the true minimum drag occurs at a small but nonzero trailing-edge thickness. It also indicates that trailing-edge thicknesses on the order of 0.5% can be utilized with drag penalties as low as one drag count. This 1981 base drag study reinforced the notion discussed in Ref. 4 concerning the advantage of using a blunt trailing edge.

The second part of the 1981 study involved the evaluation of potential trailing-edge modifications of an existing transport wing geometry. The original wing section in this case predated the supercritical airfoil and has a conventional positive included angle closure. The design objective for the study was to introduce some level of aft camber near the trailing edge of this section and to make a corresponding improvement in the transonic lift and drag characteristics. In other words, find a modest change to the trailing-edge region that would achieve some measure of the supercritical airfoil performance without having to redesign the entire wing.

The trailing edge of the original airfoil section is shown in Fig. 5. Three possible trailing-edge modifications are also shown in Fig. 5. Although all three shapes would add aft-camber effect to the airfoil section, the small reversed wedge with no chord extension was the most intriguing configuration. The wedge added to the lower surface was intriguing in several respects. First, the base drag study had indicated that the base drag for such a wedge would be acceptable if its size was kept small. Second, of the three approaches, the added lower surface wedge was the most easily accomplished for wind-tunnel model testing. Third, the added wedge seemed like a natural high-speed version of the Zaparka Flap[8] or the Gurney Flap,[9] which had been demonstrated to produce surprisingly large increments in lift[9] at low-speed conditions.

A preliminary computational assessment of this configuration was made, using *Pgm H*, to evaluate the benefit of such a modification. The computations, shown in Figs. 6 and 7, reveal a strong camber effectiveness at transonic normal airfoil design conditions. "Normal" in this context implies perpendicular conditions associated with simple sweep theory. The calculated pressure distributions for the original and mod-

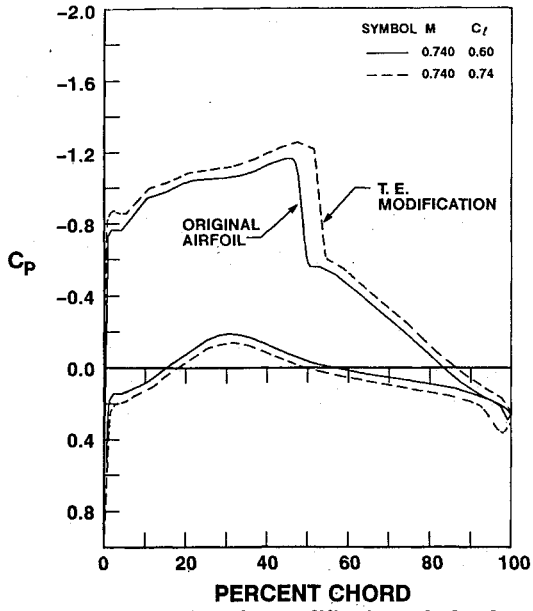

Fig. 6 DSMA 661 trailing-edge modification calculated chordwise pressure distribution at 2.2-deg angle of attack, $R_c = 14.5 \times 10^6$.

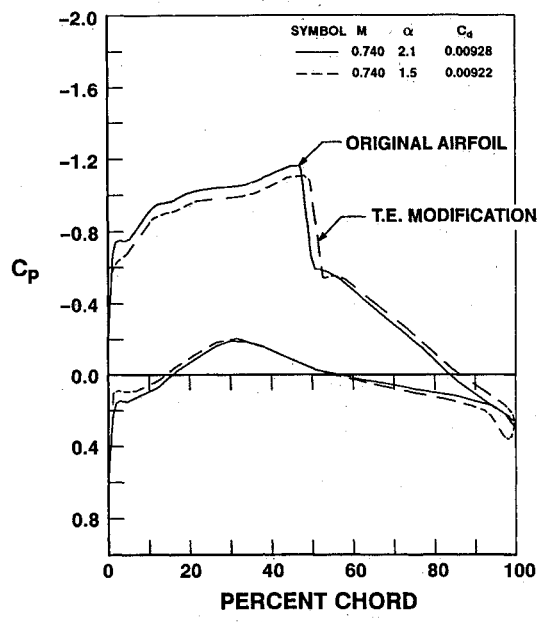

Fig. 7 DSMA 661 trailing-edge modification calculated chordwise pressure distribution at 0.6 lift coefficient, $R_c = 14.5 \times 10^6$.

ified airfoils at constant angle of attack are shown in Fig. 6. The normal Mach number is 0.74. The effect of the trailing-edge modification is a substantial increase in circulation, as can be noted by the change in velocity everywhere around the airfoil. The calculated increment in lift at constant angle of attack is 0.14, a large change in lift for transonic airfoil design. If the airfoils are compared at the same lift coefficient, as in Fig. 7, the angle of attack of the modified airfoil is less than that of the original airfoil. The results shown in Fig. 7 indicate the circulation effect and angle-of-attack effect combine to give a redistribution of the airfoil loading and a reduction of shock strength at constant lift coefficient. The reduced shock strength more than compensates for the increased base drag. The calculated lift and drag increments due to the trailing-edge modification are indicated in Fig. 8. This simple trailing-edge modification improved the airfoil lift capability and delayed the drag rise onset to higher lift coefficients.

The calculated performance improvement of the airfoil in the transonic range was impressive enough that a transonic wind-tunnel test was conducted to verify the results. The testing was accomplished in the NAE High Reynolds Number Two-Dimensional Test Facility[10] in Ottawa, Canada. The testing did verify the calculated results, as shown in Figs. 8–10. The measured pressure distributions shown in Figs. 9 and 10, at constant angle of attack and constant lift coefficient, respectively, indicate the same character as the original computations shown in Figs. 6 and 7. The measured lift and drag increments, due to the trailing-edge modification, match the calculated increments remarkably well, as indicated in Fig. 8.

The airfoil performance improvement identified for this small modification was gratifying, but, more importantly, the effectiveness of this modification caused a re-examination of trailing-edge design approaches.

Development of the DTE Airfoil Concept

Computational Development

The 1981 test substantiated the computationally predicted effectiveness of small variations in airfoil contour near the trailing edge. In order to exploit this effect, a large study of various approaches to trailing-edge contouring was accomplished. The key to the study was to recognize that a thick trailing edge is acceptable and admits closures with negative included angles and that sharp curvature near the trailing edge is acceptable. This recognition is nothing less than discarding traditional closure principles. The results of this exhaustive computational effort led to the development of the DTE concept.

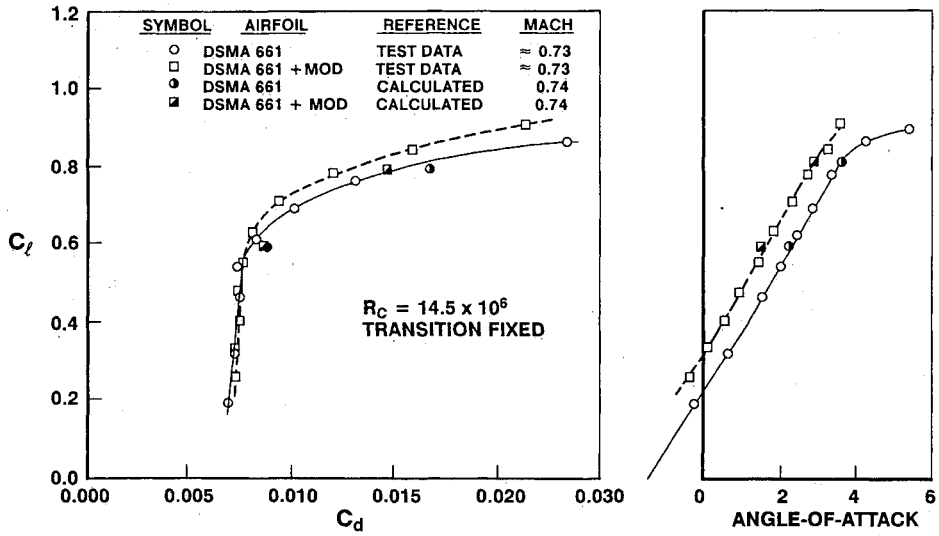

Fig. 8 Comparison of calculated and measured lift and drag characteristics for DSMA 661 modification.

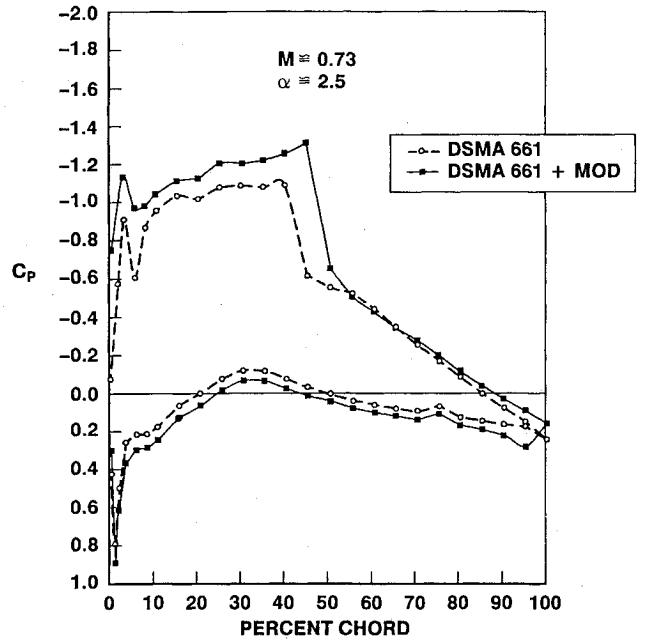

Fig. 9 Measured effect of trailing-edge DSMA 661 pressure distributions at constant angle of attack, $R_c = 14.5 \times 10^6$.

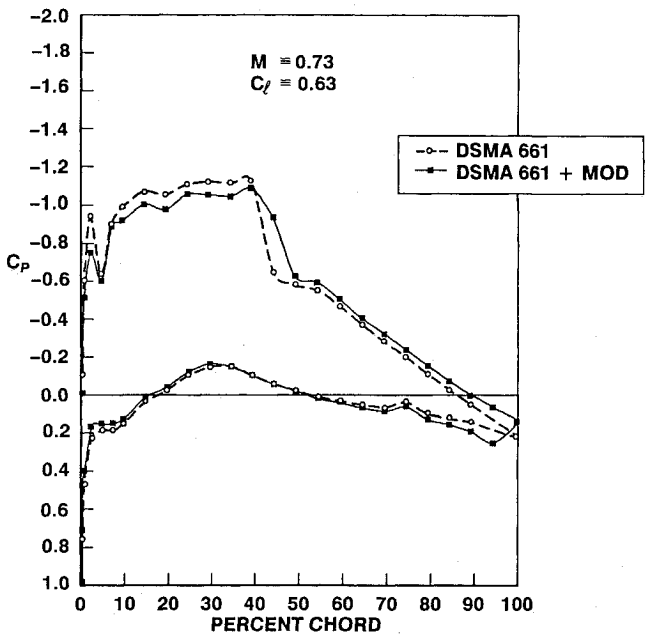

Fig. 10 Measured effect of trailing-edge modification on DSMA 661 pressure distributions at constant lift, $R_c = 14.5 \times 10^6$.

The context of the trailing-edge contouring study was advanced airfoils for transport aircraft application. Consequently, the starting point was a well-developed supercritical airfoil section. As indicated in Fig. 11, a baseline or original airfoil was used to initiate a series of parametric variations. The variations shown in the figure represent lower surface contour changes very near the trailing edge. Two constraints must be observed in this process. First, it is important to maintain sufficient structural thickness in this region to make a practical design. Second, the lower surface contouring can create adverse pressure gradients sufficient to cause lower surface boundary-layer separation. This condition needs to be avoided in the operational lift range of the airfoil section.

Results shown in Fig. 12 are presented to generalize some of the computational study efforts using *Pgm H*. In this figure, total section drag is plotted vs trailing-edge included angle for a large number of airfoils derived from a baseline airfoil DLBA 186. The normal Mach number of 0.74 and the normal lift coefficient of 0.8 are typical design conditions for advanced airfoil designs. Each data point represents a discrete airfoil configuration that was computationally designed and analyzed in detail. The objective of the study was to determine the best trailing-edge closure for minimum drag without the traditional trailing-edge design constraints. As indicated, the trailing-edge included angles of interest are negative and represent upper and lower surfaces that strongly diverge from each other. At any given trailing-edge angle, some variation is noted with different lower surface contours. Several constraint limits are also indicated in the figure. Two lower surface boundary-layer separation boundaries are shown. The Nash-Macdonald method calculation[11] is known to be conservative in the determination of separation; therefore, this boundary offers some design margin, for example, to lower lift coefficients. The second separation limit is a Cebeci method calculation.[12] This calculation of separation is typically more accurate. The third constraint is the structural thickness limit. Airfoils beyond this line have a minimum thickness point that is not sufficient for practical structure for the typical transport application. Determination of this constraint is dependent upon the application and the aggressiveness of the structural designer. The results shown in the figure indicate that drag reductions on the order of 11% were obtained for airfoil sections in the -20 to -25 deg range. Such a performance improvement at an airfoil design point is quite substantial and was unexpected.

The airfoil geometry that is indicated as DLBA 243 is compared to the baseline DLBA 186 in Fig. 13. A close-up view of the trailing edge is also shown. In this case, the upper surfaces of the two airfoils are identical. The lower surfaces differ predominantly near the trailing edge, where the DTE has been cut into the contour of the original airfoil. It is apparent in the blowup view that the upper and lower surface divergence is substantial, and there is a rapid increase in lower surface curvature as the trailing edge is approached. However, in

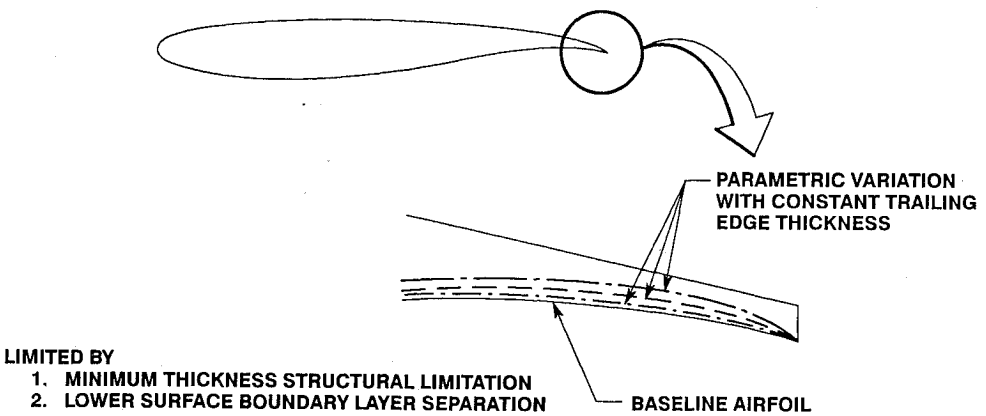

Fig. 11 Divergent trailing-edge airfoil concept development.

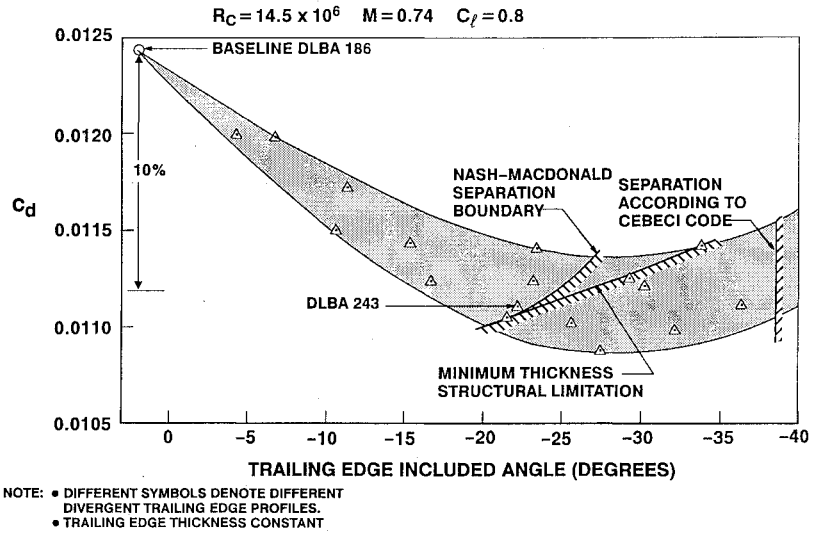

Fig. 12 Effect of divergent trailing-edge profiles on calculated airfoil total drag coefficient.

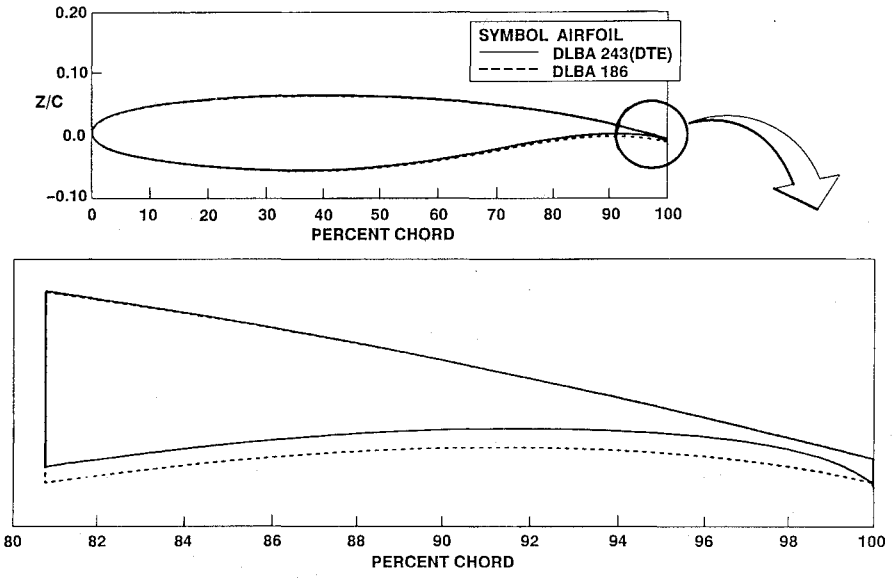

Fig. 13 Comparison of DLBA 243 and DLBA 186 airfoil sections.

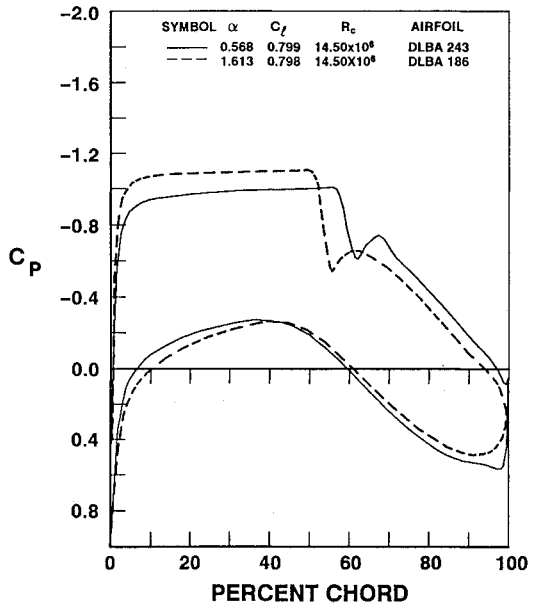

Fig. 14 Comparison of DLBA 243 (DTE) and DLBA 186 calculated chordwise pressure distributions at 0.74 Mach number.

observing the view of the complete airfoil, it is hard to say that a significant change has been made at all.

Calculated pressure distributions for these two airfoils at the design point Mach number of 0.74 are compared in Fig. 14. The lift coefficient for both is 0.8. It is clear in this comparison that the airfoil loading near the trailing edge has been substantially altered. A very large incremental C_p is maintained to essentially the trailing edge. In other words, the lower surface high pressure is held to very near the trailing edge, and the upper surface low pressure is also maintained to the trailing edge. The upper surface adverse gradient is reduced, whereas the lower surface gradient is increased. The character of the DTE provides an uncoupling of the upper surface from the lower surface. The flow along each surface can be designed to produce a more balanced upper surface and lower surface level of work at the same operating condition. The upper surface pressure distribution can be designed to terminate at one C_p level, whereas the lower surface pressure distribution can be designed to terminate at a completely different C_p level. This uncoupling of the two surfaces is facilitated by the high curvature and divergence in the geometry of the trailing edge. The lower surface flow is required to go through very rapid turning and acceleration to affect flow closure beyond the airfoil physical trailing edge.

The trailing edge C_p that is achieved by the DTE airfoil is between 0.1 and 0.15 more negative than the original airfoil. This effect is due to the combination of the trailing-edge thickness and divergence. If this variation in trailing-edge pressure level is considered in canonical pressure distribution form,[13] the ability to recompress and terminate the airfoil suction surface at a much lower pressure offers numerous airfoil design opportunities.

This implementation of the DTE introduces a significant increase in circulation at a given angle of attack. As a result, the comparison at constant lift coefficient, shown in Fig. 14, indicates a significant reduction in shock strength associated with reduced angle of attack. It should also be noted that airfoil pitching moment coefficient for this implementation is approximately 0.04 more negative.

The calculated drag rise characteristics of the two airfoils are compared in Fig. 15. The advantage of the DTE at the design point is roughly a 0.0014 reduction in drag coefficient, an 11% reduction in section drag. Such a reduction is considered quite remarkable. At lower lift coefficients the difference is small. This drag comparison indicates that the DLBA 243 type of implementation provides an airfoil design with higher lift or camber effectiveness; that is, low drag levels are maintained to higher lift levels. The special contouring and final divergence of the DTE produces the increased camber effectiveness in the airfoil design.

Airfoil designers recognize that increased camber effectiveness can be utilized to reduce compressibility drag at a given lift, to increase lift at a given angle of attack, to increase section thickness at given lift and drag, to increase drag divergence Mach number at given lift and drag, or to produce some combination of these preceding improvements. As a result, the DTE effectiveness can be used in several ways to develop an airfoil design. In the preceding example, the DTE was used to minimize drag at a given lift.

A second example is included to illustrate a different implementation of the DTE. In this second example, the camber effectiveness of the DTE is traded for substantial improvements in the airfoil thickness in the flap region; that is, improved airfoil geometric characteristics to aid structural design considerations. The DLBA 238 DTE airfoil was designed to be aerodynamically equivalent to an original airfoil designated DLBA 032. In this design the trailing-edge thickness, maximum thickness, and upper surface contour were constrained to be the same as the original DLBA 032 section. The effective camber increase of the DTE was offset by increasing airfoil depth from approximately 50 to 95% chord along the lower surface. The DLBA 238 and DLBA 032 section geometries are

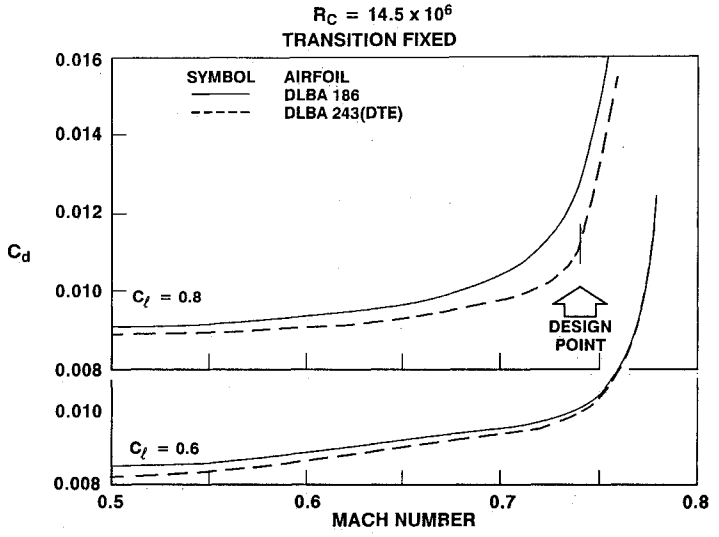

Fig. 15 Comparison of DLBA 243 and DLBA 186 calculated drag rise characteristics.

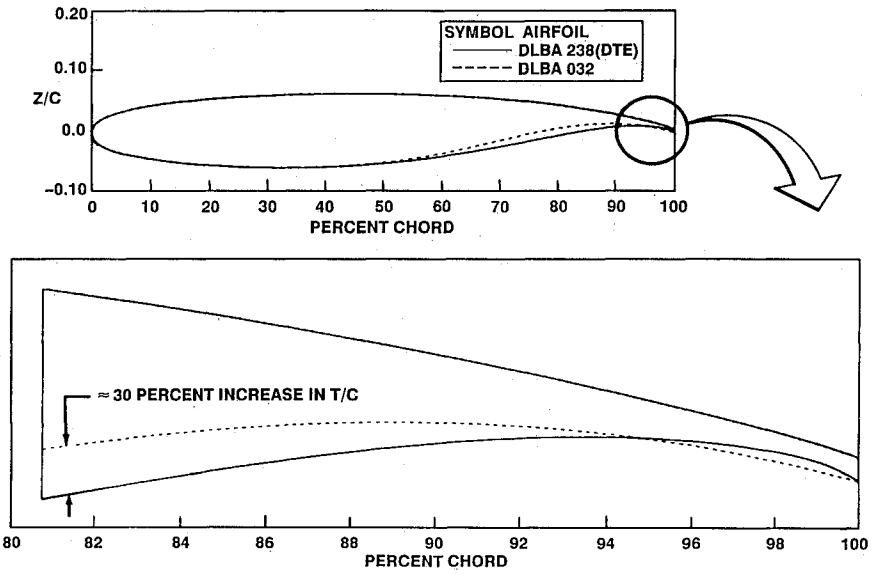

Fig. 16 Comparison of DLBA 238 and DLBA 032 airfoil sections.

compared in Fig. 16. The substantial increase in airfoil depth in the flap spar region, 70–80% chord, is quite evident. The DLBA 238 is roughly 30% thicker in this region.

The calculated pressure distributions for DLBA 238 and DLBA 032 are shown in Fig. 17 for the design point conditions. The upper surface pressure distribution is nearly the same for both airfoils. The only notable exception is the slightly lower pressure along the upper surface near the trailing edge. However, considerable difference is noted in the lower surface pressure distributions. The increased velocities from approximately 56 to 94% relate roughly to the region of increased airfoil depth. The lower surface recompression gradient has been made nearly linear.

Figure 18 illustrates the calculated drag rise characteristics of the two sections at 0.6 and 0.8 lift coefficient. The characteristics are matched at the design point and within computational (and experimental) accuracy elsewhere. Nearly identical lift and moment characteristics were also calculated. If the geometric changes illustrated in Fig. 16 are considered in light of the performance equivalence shown in Fig. 18, the camber loss from 50 to 95% chord is offset by the camber increase from 95 to 100% chord. The ratio of these chordwise extents is a measure of the surprising effectiveness of the DTE concept.

Experimental Evaluation

The DLBA 243 and DLBA 238 DTE airfoils, as well as their baseline sections, were wind tunnel tested to experimentally verify the concept and to establish an experimental database. The wind-tunnel tests were accomplished at the NAE facility. Special fabrication and inspection precautions were taken to insure that the details of the DTE were physically reproduced at model scale.

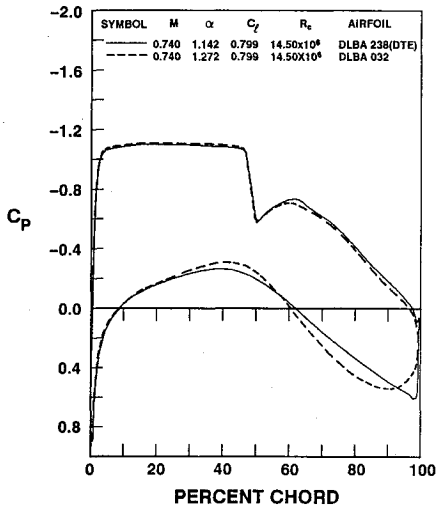

Fig. 17 Comparison of DLBA 238 and DLBA 032 calculated chordwise pressure distributions.

The measured pressure distributions for DLBA 186 and DLBA 243 are shown in Fig. 19. If Fig. 19 is compared to Fig. 14, the measured pressure distributions reproduce the calculated pressure distributions quite well. More importantly, it can be noted that the incremental effects of the DTE implementation are well substantiated in the measured results.

The measured drag rise characteristics for DLBA 186 and DLBA 243 are illustrated in Fig. 20. At the design point, these data indicate a drag reduction of nearly 0.0020. If these measured results are compared to the calculations shown in Fig. 15, the measured design point drag improvement is slightly better than expected. At lower lift coefficients the drag characteristics are essentially the same, as was expected. Perhaps as important is the continued increase in drag improvement at lift coefficients higher than 0.8. At 0.85 lift coefficient, the DLBA 243 drag characteristics are still remarkably good.

These measured aerodynamic characteristics match the predicted characteristics quite well. The incremental performance improvement of the DTE is validated by these measurements. The magnitude of the improvement in aerodynamic performance is considerable and represents a step in technology beyond the supercritical airfoil.

The second airfoil series, DLBA 032 and DLBA 238, was also successfully tested. The design point pressure distributions are illustrated in Fig. 21. If Fig. 21 is compared to Fig. 17, the alteration of the lower surface recompression by the DTE implementation is clearly indicated. The similarity in the upper surface pressure distributions is also recognized.

The DLBA 238 airfoil was designed to have matched lift and drag characteristics at the design point by trading the DTE camber effectiveness for substantially increased airfoil aft thickness. The measured lift curve and drag polar characteristics shown in Fig. 22 confirm that the design trade was successful. The drag polar comparison reveals that the DLBA 238 DTE airfoil actually has slightly less drag at the 0.8 lift coefficient design point. Additionally, the lift curve indicates that at a constant angle of attack the DTE airfoil produced slightly higher lift than the original airfoil. This incremental lift indicates that a small portion of the increased camber effectiveness of the DTE was retained and not traded away. The lift curve comparison indicates this increment is essentially preserved through buffet onset and up to high-speed stall.

This second set of airfoils, utilizing a different implementation of the DTE concept, represents an independent confirmation of the fundamental advantage of the DTE. The interesting aspect of this second set is the introduction of the design

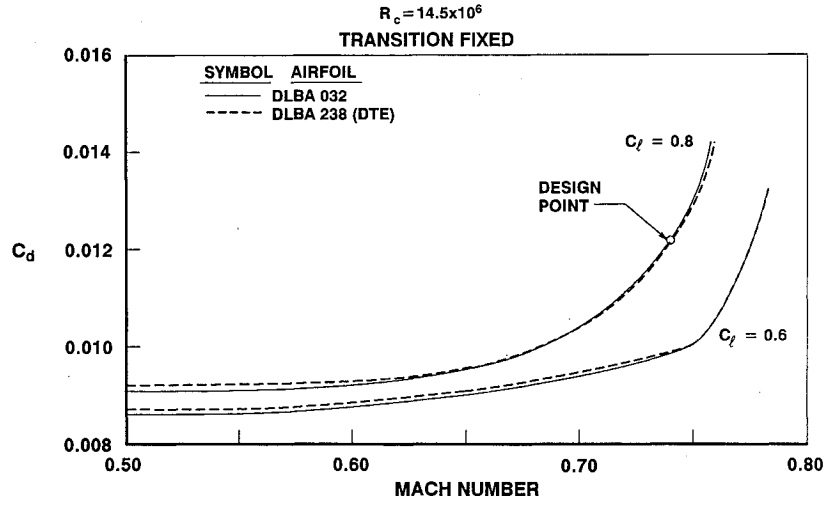

Fig. 18 Comparison of DLBA 238 and DLBA 032 calculated drag rise characteristics.

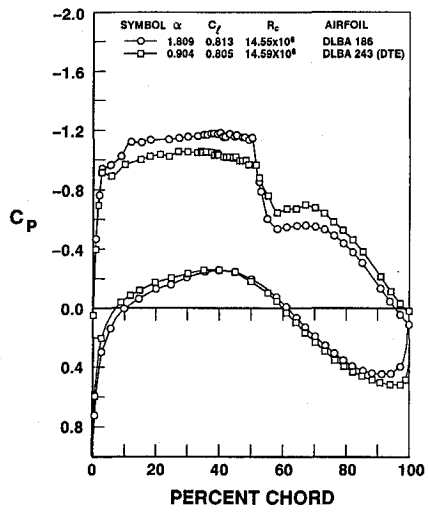

Fig. 19 Comparison of DLBA 243 and DLBA 186 measured chordwise pressure distributions at 0.74 Mach number.

trade in conjunction with the DTE. The airfoil designer can contemplate the DTE as an additional degree of design freedom or flexibility not previously recognized.

The basic aerodynamic traits associated with the DTE include increased camber effectiveness, reduced upper surface trailing-edge recompression pressure level, increased lower surface recompression pressure very near the trailing edge, and aft loading carried essentially to the trailing edge. With regard to the latter characteristics, it is interesting to consider the DTE and the Kutta condition. Clearly, the upper and lower surface pressure distributions are matched to some condition, perhaps equivalence, near the trailing edge. However, the gradients in pressure near the DTE lower surface are necessarily very large in both the chordwise and normal directions. Such gradients render definition of the Kutta condition a bit more speculative for the DTE than for previous configurations.

Wing Application of DTE Airfoils

In addition to airfoil design and testing, a complete wing development effort was also conducted in order to address any issues that might arise from a three-dimensional swept-wing design application of the DTE concept. A high-performance supercritical wing configuration that was previously developed for an advanced commercial transport application was used as a baseline configuration. This configuration, designated W_7, was designed computationally using the methods outlined in Ref. 5. These methods included the Douglas version of Jameson's FLO22 and the inverse transonic wing design method.[14] The design Mach number of the wing was 0.77. The baseline W_7 was well-developed computationally to include tailoring for not only high-speed cruise efficiency but also for low-speed high-lift conditions, for low-speed stall characteristics, for high-speed buffet lift conditions, for high-speed pitch characteristics, for surface curvature producibility considerations, and for nacelle/pylon integration. This configuration had also been experimentally validated. In short, the aerodynamic definition was complete and ready for full-scale development.

This wing was computationally redesigned with an implementation of the DTE concept. The implementation used for this wing, designated W_{15}, was the same as for the DLBA 243 airfoil. The objective of the design was to minimize drag at a given design lift. Constraints were imposed to maintain constant planform, constant spanload distribution, and constant spanwise distribution of airfoil maximum thickness, and to retain all of the tailored features of the baseline wing configuration. The planform for the baseline W_7 wing and the W_{15} DTE wing is shown in Fig. 23. With the imposed constraints, the inviscid induced drag is held constant. Hence, the objective was to implement DTE airfoil sections into the design and achieve a reduction primarily in shock drag for the wing.

The tail-off design lift coefficient range for this wing is 0.55–0.6. The calculated improvement in compressibility drag, defined as the variation in drag above the level at 0.5 Mach number, is illustrated in Fig. 24. The calculated drag coefficient improvement at 0.77 Mach number and 0.55 lift coefficient is .0005. At 0.6 lift coefficient, the DTE improvement is .0010. This latter increment is roughly 3% of aircraft drag for the original transport aircraft application. This predicted improvement is significant and prompted a wind-tunnel test to validate the results.

A wind-tunnel test of both wings was conducted in the Rockwell International Seven Foot Trisonic Wind Tunnel in El Segundo, CA. Both wings were mounted to a representative fuselage. The test Reynolds number was approximately 3.6 million, based on wing mean aerodynamic chord (MAC). At this subscale Reynolds number, care was taken to set transition on the wing upper and lower surfaces so that high Reynolds number drag characterisitics could be simulated.[5] This transition position also insured that the lower surface boundary layer was not overly thickened in the region of the DTE.

The measured DTE improvement in compressibility drag is presented in Fig. 25. At the 0.77 Mach number design conditions, the drag increments are quite close to the computations illustrated in Fig. 24. Further, the trend of continued improve-

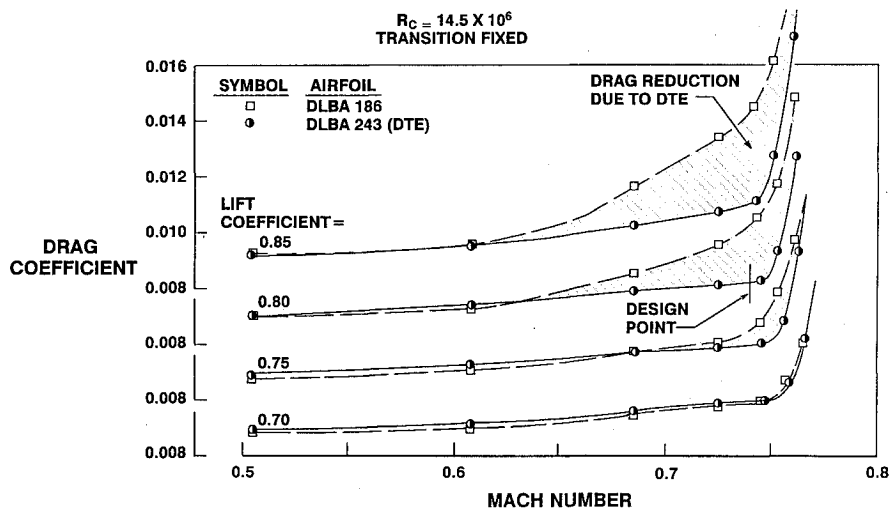

Fig. 20 Measured drag characteristics for DLBA 243 and DLBA 186.

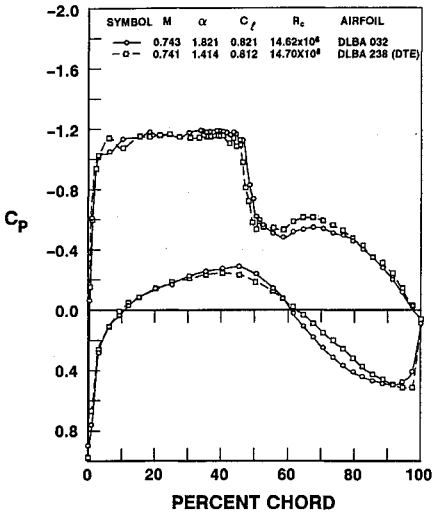

Fig. 21 Comparison of DLBA 238 and DLBA 032 measured chordwise pressure distributions.

ment at higher lift coefficients, which was identified in the DLBA 243 airfoil characteristics, is also evident in this wing comparison. In fact, the W_{15} DTE wing drag rise character at the very high-lift coefficient of 0.7 is still remarkably well-behaved.

A more complete set of three-dimensional wing characteristics, including drag polars, pitching moment, and buffet lift coefficients, is described in Ref. 15. See also Ref. 16 for additional DTE wing studies.

Wing/body lift-to-drag ratio effects are compared in Fig. 26. The L/D characteristics at 0.77 Mach number indicate that at peak L/D an improvement of over 4% has been achieved with implementation of the DTE concept on this wing configuration. Such an improvement in aerodynamic efficiency is quite substantial. Early studies of supercritical airfoil technology[17] identified aerodynamic efficiency improvements of 5–10% for application of high-aspect-ratio supercritical wings when compared to lower aspect-ratio conventional wings. If the conventional wing aspect ratio was equivalent to that of the supercritical wing then about half that advantage is lost. By comparison, the improvement measured for the DTE is roughly the same magnitude. Hence, it

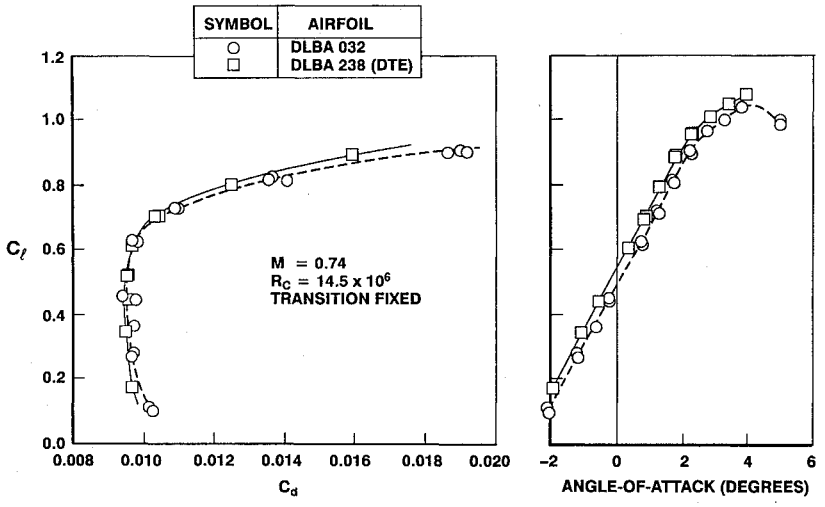

Fig. 22 Comparison of DLBA 238 and DLBA 032 measured lift curve and drag polar characteristics.

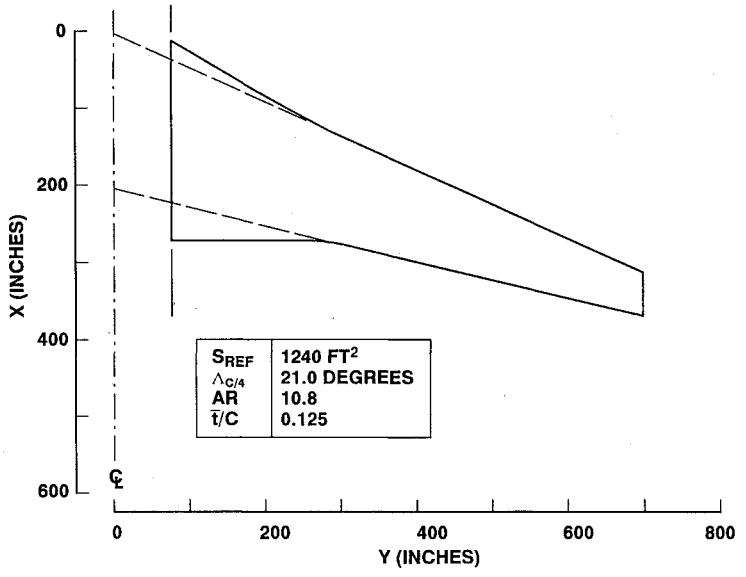

Fig. 23 Planform definition for wings W_7 and W_{15}.

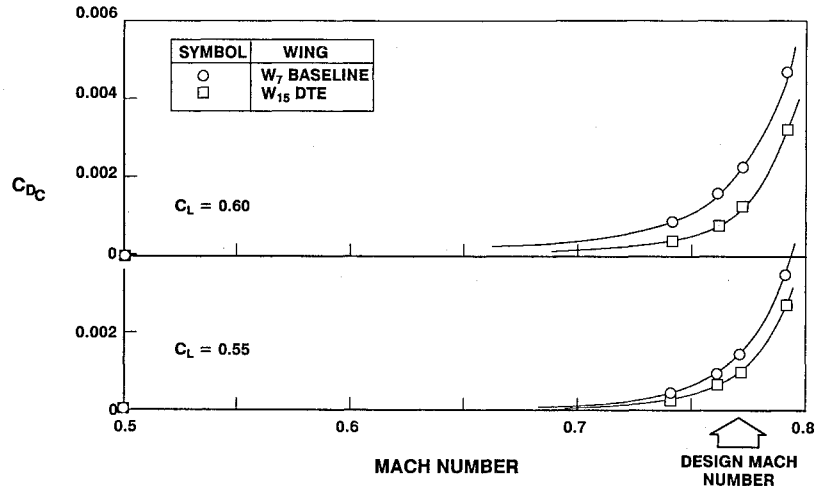

Fig. 24 Comparison of calculated compressibility drag characteristics for supercritical wing W_7 and DTE wing W_{15}.

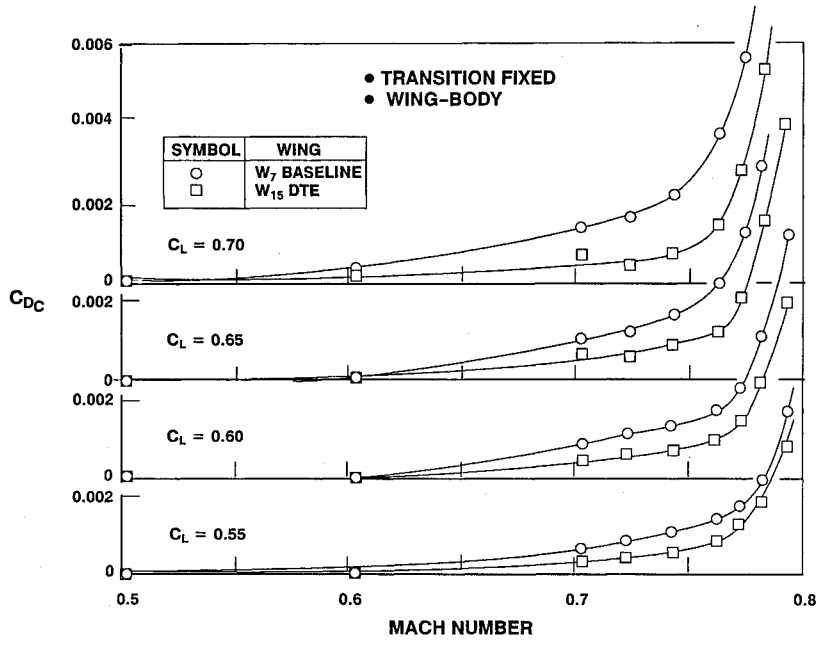

Fig. 25 Comparison of measured compressibility drag characteristics for supercritical wing W_7 and DTE wing W_{15}.

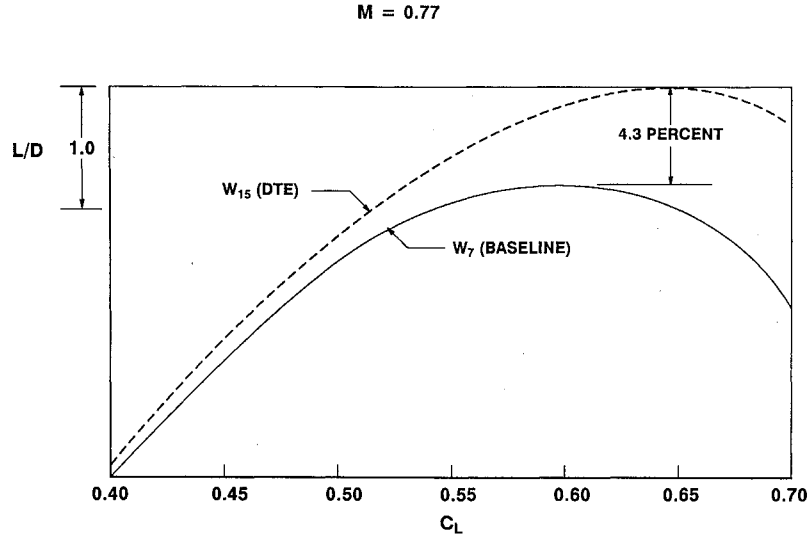

Fig. 26 Comparison of measured wing/body L/D characteristics.

has been demonstrated that the DTE represents an advancement in airfoil technology beyond that achieved with the supercritical airfoil.

Summary and Conclusions

A new concept in airfoil design has been developed. The concept, referred to as the divergent trailing edge (DTE) airfoil, utilizes unconventional trailing-edge closure geometric characteristics. These characterisitics include a finite trailing-edge thickness, strongly divergent trailing-edge upper and lower surfaces, and high surface curvature on the lower surface at or near the trailing edge.

The inception and development of the DTE was accomplished as a result of airfoil trailing-edge design investigations utilizing a computational aerodynamics method as the tool. It is very unlikely that the DTE would have been discovered without the availability of such a method. The computational development of the DTE led to the recognition that traditional airfoil closure principles could be abandoned. In doing so, airfoil performance limitations inherent in the traditional principles are also abandoned.

Two different implementations of the DTE in airfoil designs have been demonstrated. In the first case, DLBA 243, the increased camber effectiveness of the DTE was utilized to develop an airfoil design with much superior transonic lift and drag characteristics than was previously attainable. In the second case, DLBA 238, the DTE camber effectiveness was traded for improved geometric characteristics while holding aerodynamic performance essentially constant. Both airfoils were computationally designed and wind tunnel tested to validate the DTE design concept. Both examples were quite successful in achieving the design objectives. The two different approaches for the use of the DTE also encourage the airfoil designer to consider yet other applications. The ability of the DTE to decouple the upper and lower surface pressure distributions near the trailing edge offers new possibilities for the designer.

The confidence established by the airfoil development naturally led to a wing design application to insure that any three-dimensional design issues were addressed for a DTE application. A wing design was computationally developed utilizing a DTE implementation very similar to that used in DLBA 243. The calculated aerodynamic performance improvement was large and was confirmed in subsequent wind-tunnel testing. The DTE performance improvement, compared to a contemporary supercritical wing, is similar in magnitude to the improvement originally associated with the supercritical wing. Hence, the DTE represents an advancement in airfoil aerodynamic technology. It is clear that this concept provides the aerodynamicist an additional degree of design freedom and flexibility previously unrecognized.

Acknowledgment

This work was supported by the McDonnell Douglas Independent Research and Development (IRAD) Program. Partial support for the testing of the DLBA 238 airfoil was provided by NASA Langley Research Center under Contract NAS1-15327.

References

[1]Abbott, I. H., and Von Doenhoff, A. E., *Theory of Wing Sections,* Dover, New York, 1959.

[2]Hoerner, S. F., *Fluid-Dynamic Lift,* Hoerner Fluid Dynamics, Brick Town, NJ, 1975.

[3]Whitcomb, R. T., "Review of NASA Supercritical Airfoils," *Proceedings of the Ninth International Congress of the International Council of the Aeronautical Sciences (ICAS),* 1974.

[4]Harris, C. D., "Wind Tunnel Investigation of Effects of Trailing Edge Geometry on a NASA Supercritical Airfoil Section," NASA TM-X-2336, 1971.

[5]Henne, P. A., Dahlin, J. A., and Peavey, C. C., "Applied Computational Transonics—Capabilities and Limitations," *Transonic Aerodynamics,* Vol. 81, Progress in Astronautics and Aeronautics, AIAA, New York, 1982, pp. 511–543.

[6]Bauer, F., Garabedian, P., Korn, D., and Jameson, A., *Supercritical Wing Sections II,* Lecture Notes in Economics and Mathematical Systems, Vol. 108, Springer-Verlag, Berlin, 1975.

[7]Nash, J. F., "A Review of Research on Two-Dimensional Base Flow," British Aeronautical Research Council, London, RM 3323, 1963.

[8]Zaparka, E. F., United States Patent No. 19,412, 1935.

[9]Liebeck, R. L., "Design of Subsonic Airfoils for High Lift," *Journal of Aircraft,* Vol. 15, No. 9, 1978, pp. 547–561.

[10]Ohman, L. H., "The NAE High Reynolds Number 15×60 Inch Two Dimensional Test Facility," National Research Council, Ottawa, Canada, NRA LTR-HA-4, April 1970.

[11]Nash, J. F., and Macdonald, A. G. J., "The Calculation of Momentum Thickness in a Turbulent Boundary Layer at Mach Numbers up to Unity," British Aeronautical Research Council, London, ARC CP 963, 1967.

[12]Cebeci, T., and Bradshaw, P., *Momentum Transfer in Boundary Layers,* McGraw-Hill, New York, 1977.

[13]Smith, A. M. O., "High-Lift Aerodynamics," *Journal of Aircraft,* Vol. 12, No. 6, 1975, pp. 501–530.

[14]Henne, P. A., "Inverse Transonic Wing Design Method," *Journal of Aircraft*, Vol. 18, No. 2, 1981, pp. 121–127.

[15]Henne, P. A., and Gregg, R. D., III, "A New Airfoil Design Concept," AIAA Paper No. 89-2201, July 1989.

[16]Gregg, R. D., III, Hoch, R. W., and Henne, P. A., "Application of Divergent Trailing-Edge Airfoil Technology to the Design of a Derivative Wing," Society of Automotive Engineers, Warrendale, PA, SAE Paper 892288, 1989.

[17]Steckel, D. K., Dahlin, J. A., and Henne, P. A., "Results of Design Studies and Wind Tunnel Tests of High Aspect Ratio Supercritical Wings for an Energy Efficient Transport," NASA CR 159332, Oct. 1980.